

Testing the 2020 European Seismic Hazard Model (ESHM20) against observations from Romania

1 Elena F. Manea^{1,2}, Laurentiu Danciu³, Carmen O. Cioflan¹, Dragos Toma-Danila¹, Matthew C.
2 Gerstenberger²

3 ¹ National Institute for Earth Physics, Măgurele, 077125, Ilfov, Romania

4 ² GNS Science, PO Box 30-368, Lower Hutt, New Zealand

5 ³ ETH Zurich, Seismology and Geodynamics, Sonneggstrasse 5, 8092 Zurich, Switzerland

6

7 *Correspondence to:* Elena F. Manea (flory.manea88@gmail.com); Laurentiu Danciu (laurentiu.danciu@sed.ethz.ch)

Abstract. Evaluating the performance of probabilistic seismic hazard models against recorded data and their potential to forecast future earthquake's ground shaking is an emerging research topic. In this study, we evaluate and test the results of the recently released European Seismic Hazard Model (ESHM20; Danciu et al., 2021, [Danciu et al 2024](#)) against observations for several cities in Romania. The dataset consists of ground shaking recordings and macroseismic observations, which extend the observational time-period to a few hundred years. The full distribution of the hazard curves, depicting the epistemic uncertainties of the hazard at the given location was considered and the testing was done for peak ground acceleration (PGA) values, ~~i.e.~~, 0.1g and 0.2g.

8 The results show ~~consistency~~ ~~close agreement~~ between the ESHM20 and the ground motion observations for the cities located
9 near the Vrancea intermediate-depth source (VRI) for both selected PGA levels. ~~ESHM20's estimated values appear~~ ~~ESHM20~~
10 ~~appears~~ to ~~be over~~ ~~overestimate~~ the VRI recorded ground motions along the Carpathian Mountain Range and
11 ~~below~~ ~~underestimate~~ those at the far-field locations outside the Carpathians, yet inside the expected model variability. Some of
12 these differences might be attributed to the uncertainties in data conversion, local site effects, or differences in the attenuation
13 patterns of the ground motion models. Our analysis suggests that the observed exceedance rates for the selected PGA levels
14 are consistent with ESHM20 estimates, but these results must be interpreted with caution given the limited time and spatial
15 coverage of the observations.

16

17 **1 Introduction**

18 Probabilistic seismic hazard analysis (PSHA) is an important framework in seismology and earthquake engineering, widely
19 used worldwide to quantify the uncertainty inherent in both the occurrence and effects of earthquakes. PSHA
20 underpins ~~underlines~~ a wide range of applications, from the development of modern seismic design building codes to seismic
21 risk assessments. It also informs various public policy and risk management strategies aimed at mitigating the impacts of
22 seismic events.

23 Despite its widespread adoption, testing the PSHA results is not straightforward. The ~~sporadic~~~~inherently random~~ nature of
24 earthquakes, coupled with ~~low rate of occurrence~~~~long recurrence periods~~, or low probabilities and high consequences events,
25 makes the empirical validation of PSHA models and results a task that would typically require observations spanning multiple
26 human lifetimes (e.g. Vanneste et al., 2018; Gerstenberger et al., 2020; Allen et al., 2023). For instance, in regions like France
27 or Germany, where the installation of accelerometric stations began in the mid-~~1990s~~~~1970s~~, the ~~availability of the instrumental~~
28 ~~records~~~~empirical data available~~ is limited to a short temporal window. Even in more seismically active regions like Italy,
29 Turkey or Greece, subject to more frequent damaging events, validating probabilistic hazard models is challenging for the
30 same reasons. In recent years, several procedures have emerged aimed at testing seismic hazard estimates against past
31 observations (e.g., Hanks et al., 2012; Marzocchi and Jordan, 2018). These procedures are typically performed at ~~short~~~~shorter~~
32 (e.g., Stirling and Gerstenberger, 2010; Tasan et al., 2014; Mousavi and Beroza, 2016; Mak and Schorlemmer, 2016; Iervolino
33 et al., 2023; Stirling et al., 2023) or ~~long~~~~longer~~ return periods (e.g., Rey et al., 2018; Salditch et al., 2020; Meletti et al., 2021),
34 depending on the aim of the application.

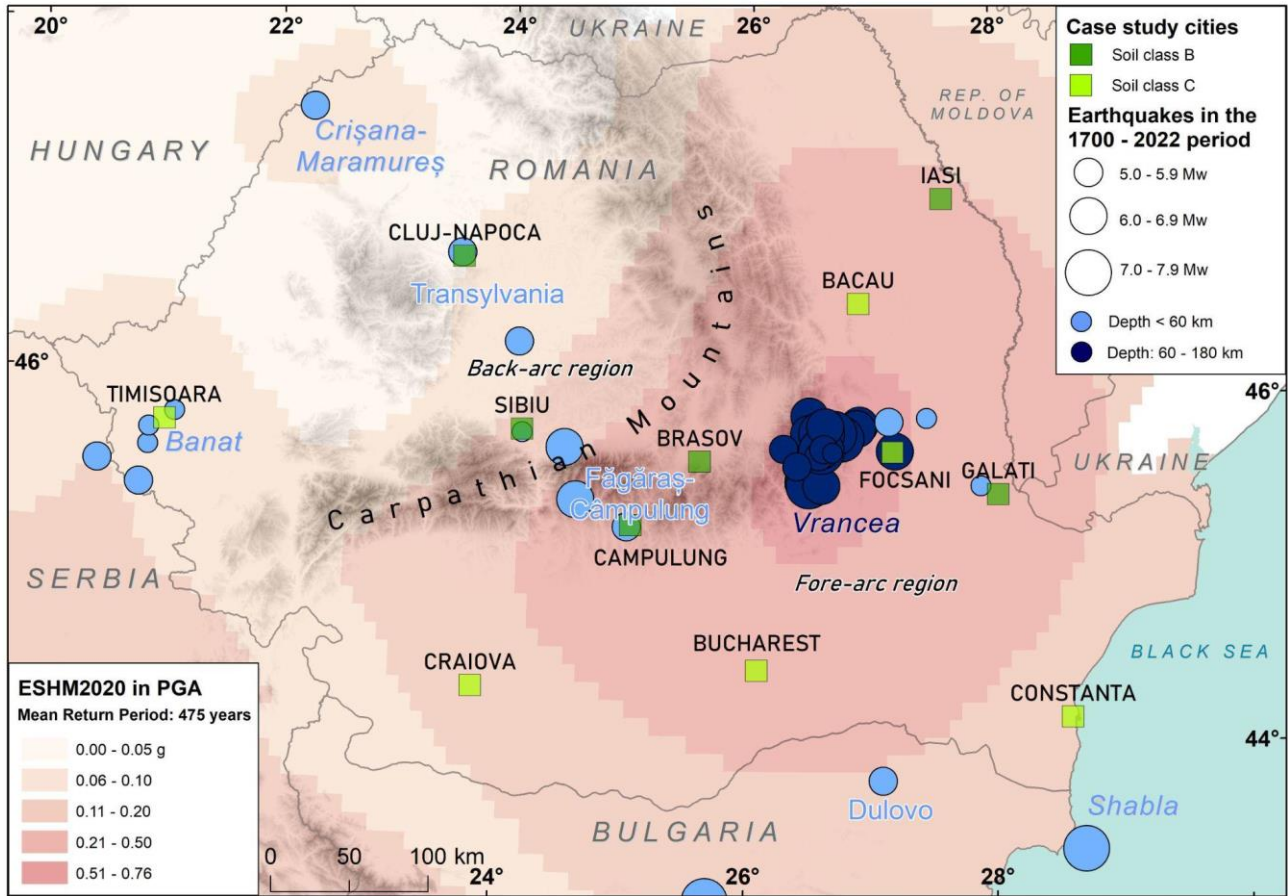
35 The current study aims to compare the recently released European Seismic Hazard Model (ESHM20; Danciu et al., 2021,
36 [Danciu et al 2024](#)) results against instrumental recordings and detailed macroseismic observations specific to Romania. This
37 region offers a distinctive seismo-tectonic landscape, dominated by the Vrancea intermediate-depth seismic source (VRI). The
38 VRI has a concentrated nest of seismicity at depths between 60 and 200 km, which is associated with the current dehydration
39 of an oceanic subducted plate, as noted by Ferrand and Manea (2021) and Craiu et al. (2022). Macroseismic intensities ~~maxima~~
40 ~~of strong VRI events are often observed/up to X Medvedev-Sponheuer-Karnik 1964 intensity scale (MSK-64, Medvedev et~~
41 ~~al., 1967) were reported, with notable/maximum effects seen~~ outside ~~of~~ the epicentral area: values of IX+ for 1940 event with
42 the moment magnitude $M_w=7.7$, and VIII+ ~~(MSK-64 scale)~~ for the 1977 event with $M_w=7.4$ (e.g. Kronrod et al., 2013).

43 -The largest intensity values are found outside of the Carpathian belt, where a substantial number of sedimentary structures are
44 located (Marmureanu et al., 2016a; 2017; Manea et al., 2019). Beside this, the source properties imprint an asymmetric shape
45 to the macroseismic field, elongating it in the NE-SW direction (Marmureanu et al., 2016b). In contrast, strong back-arc
46 attenuation features are recorded within the Carpathian region and prescribe the current pattern of the macroseismic fields (e.g.
47 Vacareanu et al., 2015; Manea et al., 2022). The VRI impact ~~extends beyond~~~~overpass~~ the national borders and significant

48 damage has been reported in neighbouring countries, ~~withe.g.,~~ observed intensities of VII-VIII at more than 250 km epicentral
49 distances during ~~the~~ 7.7Mw 1940 event (Cioflan et al., 2016).

50 -Furthermore, while the shallow crustal seismic activity in Romania is not as frequent as the one at intermediate depths in the
51 Vrancea region, it still poses a significant contribution to the regional seismic hazard ~~(-Marmureanu et al., 2016a)~~. The main
52 seismic sources for such events are located along the Carpathian Mountains, particularly in the Făgăraș-Caâmpulung zone,
53 as well as in the foreland regions of southwestern Romania, including Banat and Danubius, and extending northwest to Crisana-
54 Maramures. Despite ~~the~~ lower rate of crustal activity in these areas compared to the Vrancea region, historical accounts and
55 pre-instrumental catalogues document significant earthquakes with magnitudes $M_w \geq 5$ and epicentral intensities $I_0 \geq VI_6$ MSK
56 scale, ~~indicating substantial effects on the affected regions~~ (e.g., Radu, 1979; Oncescu et al., 1999). Thus, in this study, we
57 consider intensity data spanning over three centuries from twelve important cities in Romania (see ~~their locations in~~ *Figure*
58 ~~17A~~). These urban areas are selected for their significant population and different exposure to seismic hazard levels. The
59 present study begins with an overview of the ESHM20 and its specific relevance to Romania. It will then discuss the main
60 components of the model and the results relevant at the regional level. The next section describes the main data, the curation
61 and conversion procedure, which includes how historical macroseismic data were collected and converted into peak ground
62 acceleration (PGA) values for different Romanian cities. Subsequently, a summary of the statistical testing process will be
63 given, detailing the approaches taken to contrast the recorded seismic activity with the ESHM20 estimates. Next, the main
64 outcomes of the statistical testing at two reference values for PGA - 0.1 and 0.2 g, are illustrated and interpreted, followed up
65 by discussion and conclusions of our findings. ~~We also acknowledge the various attempts that have emerged in recent years~~
66 ~~aimed at testing seismic hazard estimates against past observations (e.g. Marzocchi and Jordan, 2018; Rey et al., 2018; Meletti~~
67 ~~et al. 2021, Stirling et al., 2023) and we try to use their experience when applying such techniques for Romania.~~

68



69

70

71

72

73

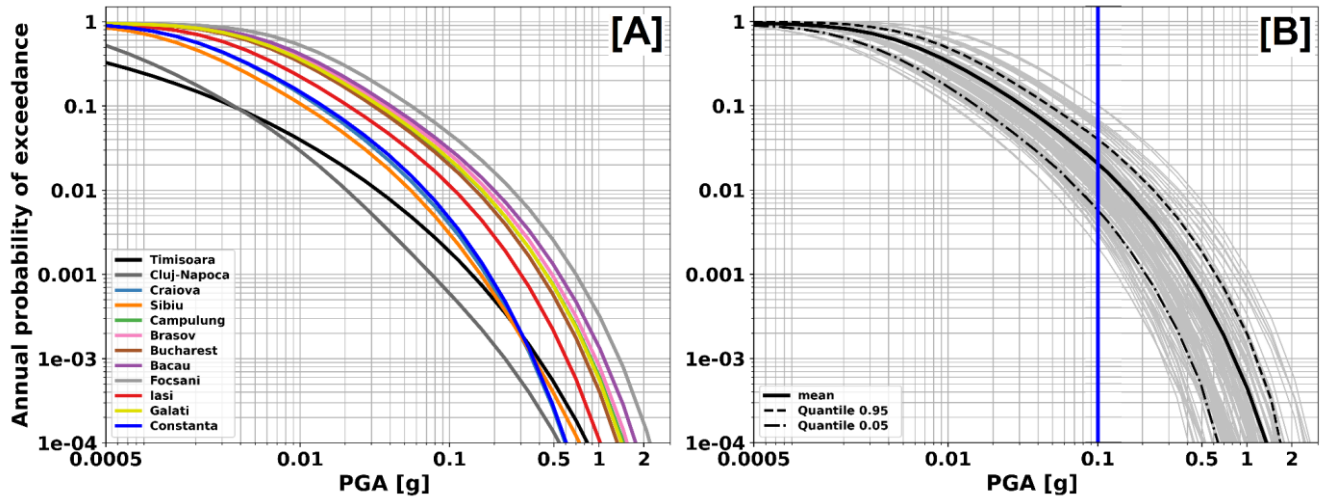
74

Figure 1: Location of the selected twelve cities and the post-1700 earthquakes (according to the Unified Earthquake Catalogues of the European Seismic Hazard Model 2020 - ESHM20; Danciu et al., 2021) used in this study. Only events with moment magnitude $M_w \geq 5$, for which at least one macroseismic intensity exceeding VI MSK-64 is recorded at the selected locations, were considered. The background is the ESHM20's ground shaking map in terms of peak ground acceleration (PGA) for a return period of 475 years.

75 2 ESHM20 Results for Romania

76 The 2020 European Seismic Hazard Model (ESHM20, Danciu et al 2021, 2022) is the latest revision and update of the seismic
77 hazard assessment for the Euro-Mediterranean region. ESHM20 is constructed using harmonised datasets that include
78 information on ground motion, earthquake catalogues, active faults, and tectonic data across different borders. The ground
79 shaking hazard in the region is estimated by combining a complex seismogenic source model, which includes distributed
80 seismicity, active faults, and subduction sources, with regionally scaled backbone ground motion models (Weatherill et al.,
81 2023). More specifically, the seismogenic source model consists of two branches of sources: the area source models and a
82 hybrid combination of active faults and background smoothed seismicity. In Romania, due to the lack of available data on
83 active faults, the seismogenic source model is based on an area source model and a smoothed seismicity with an adaptive
84 kernel. Furthermore, the seismogenic sources depicting the nested seismicity with depth in the Vrancea region are also
85 considered and modelled with a set of uniform area source zones located between 70 to 150 km depth. The ground motion
86 characteristic models for Romania are scaled based on regional factors to capture the ground shaking characteristics of both
87 the active shallow crust and non-subduction deep seismicity. These models are described by Weatherill et al., (2020, 2023). A
88 complex logic tree was developed to address the spatial and temporal variability in the earthquake rate forecast as well as the
89 regional backbone ground motion models. The computation was performed using OpenQuake (Pagani et al 2014) and the full
90 logic tree was sampled to obtain the distribution of the hazard results. For this analysis, we selected twelve major cities in
91 Romania, as illustrated in *Figure 1*, where we superimposed the ESHM20's ground shaking map in terms of peak ground
92 acceleration (PGA) for a return period of 475 years. Also, the relevant earthquakes with moment magnitude, $M_w \geq 5$ at which
93 at least one macroseismic intensity exceeding VI MSK-64 is recorded at the selected locations, are also plotted in the same
94 map. The highest PGA mean value is observed in the proximity of the Vrancea source, a region of high seismicity as indicated
95 also by the density of the seismic events (*Figure 1*). The pattern of PGA values follows the Carpathian Arc, with values
96 decreasing in the backarc towards the north-western part of the region. The range of PGA values is rather large, spanning from
97 0.15g in Cluj to 0.9 g observed for Focșani. The ESHM20's hazard curves for the mean PGA values at the selected cities in
98 Romania are presented in *Figure 2A* and show that the decay of the hazard curves is different, with a fast decay indicating
99 lower hazard and vice-versa. A significant spreading of the mean hazard curves is present between the locations outside and
100 within the Carpathian arc, following the same pattern as the 475 year mean ESHM20's ground shaking map (*Figure 2A*). The
101 highest annual probability of exceedances (APEs) is seen at locations in the proximity of the Vrancea source, which dominates
102 the hazard at all the return periods, while the lower values are observed at cities located in the far-field extent of this region,

103 where low-recurrence shallow seismicity is present. The full distribution of hazard curves for 10000 random sampled hazard
 104 curves along the ESHM20 logic tree for Bucharest is shown in *Figure 2B* together with the mean and the 5 and 95 percentiles.
 105 -At this location, the variability of the hazard curves presents a narrow range and depict the combined uncertainties of mainly
 106 the Vrancea source and ground motion (Danciu et al., 2024).
 107 Finally, we used the full distribution of the ESHM20 hazard curves to retrieve the statistical testing input, as described in the
 108 testing procedure section.
 109



110

111 **Figure 2:** [A] The ESHM20's annual probability of exceedance as a function of PGA (so called hazard curves) at the selected cities
 112 in Romania. [B] Full distribution of hazard curves for 10,000 samplings extracted across all the ESHM20 hazard branches for
 113 Bucharest city. The mean hazard is presented as a continuous black line, while the dashed ones represent the 5 and 95 percentiles.

114

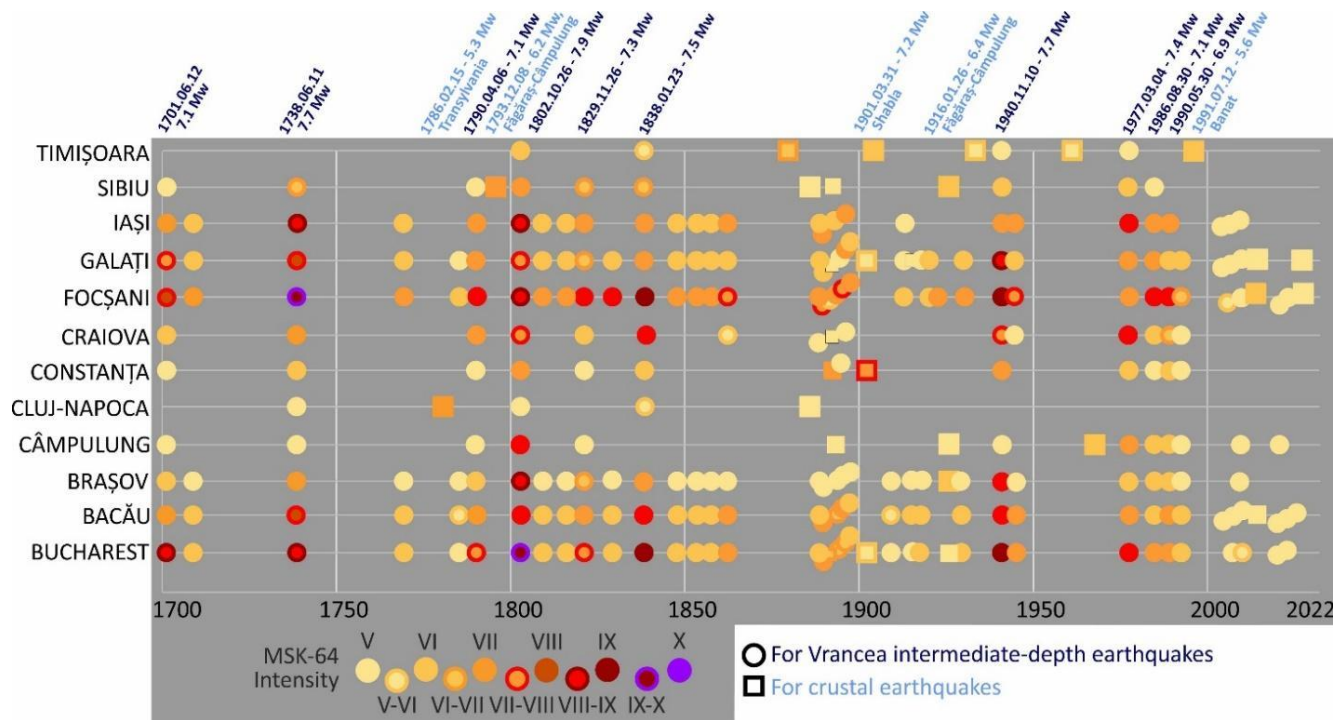
115 3 Available Data and Conversion

116 Macroseismic intensity observations recorded over several hundreds of years (starting with 1700) at the main cities across
 117 Romania are used to test ESHM20's results. The selected cities are among the most highly populated urban areas across
 118 Romania and are well-distributed with respect to the various seismic hazard levels and source characteristics shown by the
 119 ESHM20's PGA hazard map for the 475 year return period (see *Figure 1A*). It is noteworthy, that these observations were
 120 collected within this study and were not directly used in the derivation of the ground motion component of the ESHM20,
 121 securing their independence for statistical testing. Intensity data points (IDP) were acquired from multiple available sources:
 122 Atanasiu (1961), Constantin et al. (2011, 2013, 2016, 2023), Kronrod et al. (2013), Marmureanu et al. (2018), Rogoza (2014;
 123 2016) and Shebalin et al. (1974). Beside compiling original information (i.e., intensity values), most of these studies are also
 124 providing new evaluations at locations where new macroseismic information became available. Note that, while IDPs of the
 125 XVII-XVIII centuries had been evaluated from scarce information, the ones related with strong Vrancea earthquakes of the

126 20th century were collected through wide national campaigns (see details in Kronrod et al., 2013, Constantin et al., 2016).
127 Several IDPs of our initial dataset have a very local character as they strictly reflect the effects of strong intermediate-depth
128 earthquakes on specific buildings existing at the respective time (e.g. churches, monasteries; [Marmureanu et al., 2018](#)). Where
129 available, such site-specific intensity estimations are averaged with macroseismic data from other authors and various sources
130 (especially isoseismal maps). Additionally, maps published before 2000 have been checked against the information available
131 in the European Archive of Historical Earthquake Data platform (AHEAD; Rovida et al., 2020) which also helped us to fill in
132 the data gaps for some cities. If an IDP was not available at the specific location, a natural neighbour interpolation scheme
133 (Sibson, 1981) was used to extract it from georeferenced isoseismal maps selected from the above-mentioned sources. Some
134 of the collected IDPs were reported in the Rossi-Forel intensity scale (e.g., 7.1 Mw 1908 VRI earthquake) and were
135 homogenised to MSK-64 using the conversions proposed by Musson et al. (2010). Thus, we also treat MMI and EMS-98
136 intensity values as equivalent to MSK-64 ones. The MSK-64 is preferred as the VRI's intensity to ground motion conversion
137 equations (IGMCEs) were developed using this intensity scale for Romania.

138 From this collected dataset, we considered only IDP data from events with $M_w \geq 6$ for VRI and $M_w \geq 5$ for shallow seismicity
139 (see their locations in [Figure 11A](#)) and with a minimum observed epicentral intensity I_0 of VII MSK-64, which corresponds
140 to a PGA value of 112 cm/s^2 for VRI (e.g. Ardeleanu et al., 2020) and/or 154 cm/s^2 (Caprio et al., 2015) for shallow seismicity.
141 The testing dataset at the twelve major cities contains 199 IDPs recorded from 58 earthquakes (see [Figure 12](#)), from which 39
142 are located in the VRI region. For each city, the time window of data completeness (Table 1) is visually evaluated based on
143 IDPs higher or equal to V (see Figure 3) from events and are considered as mainshock/main events in the ESHM20 declustered
144 catalogue (Danciu et al., 2021; 2022). Where available, the converted PGA values were replaced by the recorded ones from
145 the postpre-1977 VRI events dataset of Manea et al., (2022). We did not include any intensity measure which is related to the
146 events identified as foreshock, aftershock, or swarm events. Depending on the available data
147 To perform a comparison between the ESHM20 results and the collected MSK-64 IDP, the intensity values were translated to
148 PGA using the latest conversion equations proposed by Ardeleanu et al., (2020) for the VRI source and Caprio et al., (2015)
149 for global crustal as no local shallow models are available. A different conversion equation was used for VRI as the observed
150 macroseismic field presents unique features which are not seen for shallow seismicity, such as: an azimuthal asymmetric shape
151 due to the source properties (Marmureanu et al., 2016b; Craiu et al., 2023), different apparent attenuation patterns due to the
152 unique tectonic environment (e.g. Manea et al., 2022) and far-field strong site effects (Cioflan et al., 2022). The equation of
153 Ardeleanu et al., (2020) was selected as it is the most recent intensity to PGA conversion equations proposed for VRI and its
154 predictions agree with the ones from the previous studies, such as Vacareanu et al., (2015) and; Marmureanu et al., (2011).
155 The distribution of the MSK to PGA conversions and their corresponding standard deviations up to X within the range of 1-10
156 MSK-64 are presented in [Figure S1](#), which can be found in the electronic *Supplementary Materials*. Each We decided to do
157 the translation from IDP was translated into three to PGA values, i.e the mean IPE model and its standard deviation, to consider
158 the variability of this conversion into the final results. The IDP was translated to PGA, as it's simply less challenging and it is

159 more efficient ~~than converting all~~to convert the relatively small number of the PGA hazard curves~~reported intensities and more~~
160 ~~importantly,~~ to intensity.
161 ~~minimises potential errors at the data levels, rather than at the results.~~ To align to the ESHM20 rock conditions, for which the
162 time-averaged shear-wave velocity to 30 m depth (V_{s30}) is set to 800 m/s, the ground-motion amplitudes were corrected for
163 site effects considering amplification in each city by means of soil factors recommended in Eurocode 8 (Comité Européen de
164 Normalisation (CEN), 2004, EC8) for crustal seismicity and the ones adjusted for Vrancea earthquakes ~~ones~~ proposed by
165 Vacareanu et al., (2014). The ~~site classification parameters, such as V_{s30} and~~ EC8 site classes, were gathered from Manea et
166 al., (2022) and Coman et al., (2020) studies and are presented in Table 1. The use of observational intensity data to compare
167 against hazard curves introduces additional layers of uncertainty. One must acknowledge the complex process of converting
168 subjective intensity measures into objective ground acceleration values, given the uncertainty nature of intensity observations
169 and the variability in the human experience of ground shaking (e.g. Rey et al., 2018). Furthermore, the determination of
170 complete and reliable historical records for specific macroseismic intensity levels is equally challenging, presenting a
171 considerable difficulty in aligning the past seismicity with probabilistic forecasts. ~~We~~To evaluate how much these uncertainties
172 ~~impact the results of the hazard testing, we~~ incorporated the full uncertainty variability within the PGA calculations by
173 considering the uncertainty on standard deviations of the conversion from intensity to PGA, to evaluate how much these
174 uncertainties impact the results of the hazard testing. ~~ground shaking conversion models.~~
175



176
177 **Figure 32:** The distribution of the selected intensity data points used for the ESHM20 hazard testing at the twelve cities, with a
178 **threshold above V MSK-64.** The timeline and primary source information for the major earthquakes, which significantly affected
179 **the Romanian territory, are presented in the upper side of the plot.**

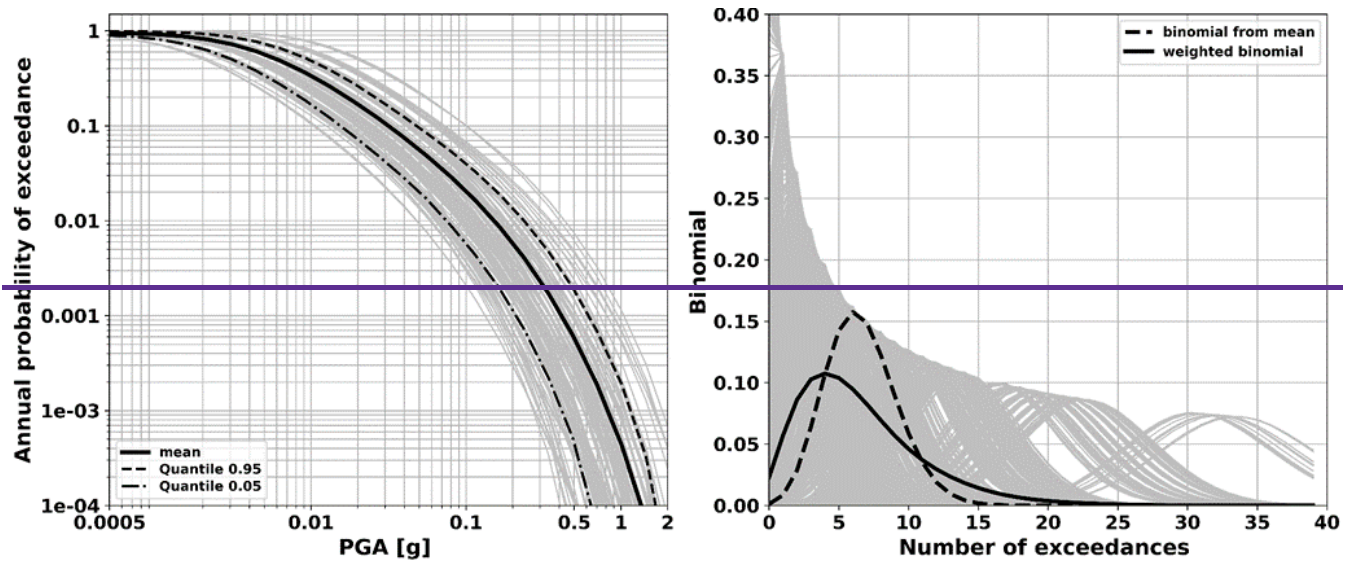
180 4 Statistical Testing Procedure

181 In the following section, we provide an overview of our methodology for evaluating the performance of the ESHM20 ground
182 shaking estimates by comparing them to instances of ground motion exceedances at twelve main cities in Romania. The
183 statistical testing relies upon comparing the actual occurrences of ground acceleration surpassing specific thresholds (0.1 and
184 0.2g PGA) with the ESHM20 estimates, by considering the associated uncertainties. The selected ground motion levels are of
185 relevance to PSHA in Romania, with 0.1g approximating the lower bound of damaging ground motions. First, we compile the
186 full dataset of ground shaking that includes both the recordings (where available) and the macroseismic observations converted
187 to PGA by considering uncertainties of the conversion process and the influence of site conditions. Next, we determine the
188 specific time period of this dataset and count the instances where the acceleration thresholds are surpassed to obtain, by
189 considering the influence of site conditions and uncertainties in the conversion process. Subsequently, we forecast the
190 anticipated number of exceeding occurrences by using a binomial distribution of the observed (Stirling et al., 2023) to evaluate
191 the likelihood of observing the exact number of exceedances over the time period of completeness.
192 This Subsequently, we follow closely the statistical testing approach follow closely the procedures proposed by Marzocchi
193 and Jordan (2014, 2017, 2018), which accounts for both the aleatory and the epistemic uncertainties of the hazard (Meleti et

194 al., 2021; Stirling et al., 2023). The above-mentioned methodology considers that the exceedance rate variability is well
195 represented by a binomial distribution. We forecast the anticipated number of exceeding occurrences for each logic-tree branch
196 by using the proposed binomial distribution (Stirling et al., 2023) and build the sum of all the weighted distributions by
197 considering each branch weight to evaluate the likelihood of observing the exact number of exceedances. 2021; Stirling et al.,
198 2023).

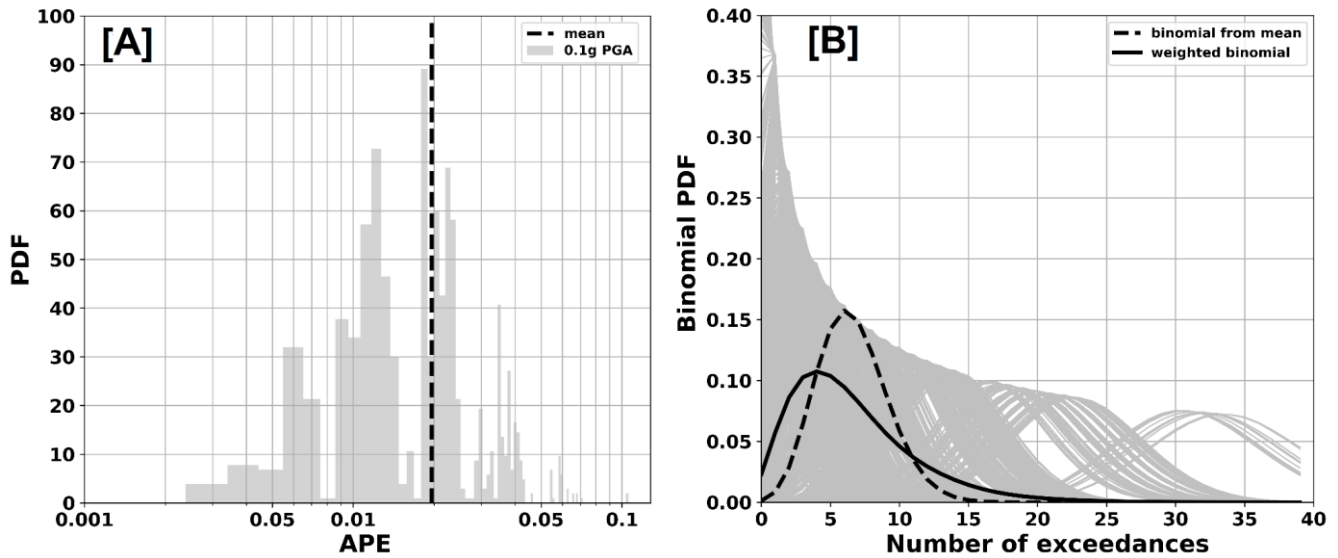
199 ~~Figure 3 illustrates the~~ The variability of the 10000 random samples of the hazard curves for Bucharest, city, the capital of
200 Romania, is presented in *Figure 2B*, while the contribution of various logic tree branches to ~~The distribution of the 10,000~~
201 ~~random sampled hazard at 0.1g PGA is illustrated~~ curves along the ESHM20 logic tree is shown in *Figure 4A*. It shows that ~~34~~
202 ~~together with~~ the mean hazard value doesn't explain the APEs asymmetric distribution. Thus, for this analysis we use ~~and~~ the
203 ~~weighted binomial distribution considering the APEs distribution of the entire ESHM20 logic tree branches~~ 5 and 95
204 ~~percentiles~~. The variability of all the computed binomials for the entire ensemble of the hazard curves are presented in *Figure*
205 *4B*, alongside the final weighted mean considering the full distribution of the uncertainties and the resulting binomial retrieved
206 from the statistical mean. ~~The distribution of the APEs reflects the contribution of various logic tree branches, and~~ Note that
207 ~~the statistics are summarized for the Annual Probability of Exceedance (APE) and that~~ the differences between the two
208 statistical descriptors i.e., weighted mean versus statistical mean is evident in *Figure 4B*. ~~To identify potential influences due~~
209 ~~to the selection of a specific distribution, we fitted several distributions to the APE range at 0.1g, as illustrated~~ *Figure S2* in
210 ~~the Supplementary Materials~~. The distribution of the APEs reflects the contribution of various logic tree branches, and given
211 ~~the fitted distribution the statistical mean, might be different~~. Thus, for this analysis we consider the weighted binomial
212 ~~distribution considering the asymmetric APEs distribution~~.

213



214

215



216
 217 **Figure 43:** [A] Probability density functions computed for 0.1g PGA level versus annual probability of exceedance - APE. Hazard
 218 curves from the 10,000 samplings extracted across all the ESHM20 hazard branches in Bucharest city. The vertical mean hazard is
 219 presented as a continuous black line indicates the traditional hazard mean value, while the dashed ones represent the 5 and 95
 220 percentiles. [B] The variability of the computed binomials for all the hazard ensemble curves (grey lines) is shown together
 221 with the final weighted mean curve considering the full distribution of the uncertainties, and the one computed from the commonly
 222 used mean hazard curve.

223
 224 Based on the above-mentioned methodology, we perform point-based assessment testing at each of the twelve cities using the
 225 following steps:

- 226
- 227 1. Estimate the time-period of available ground motion for each city in the compiled ground motion dataset (
 228 in terms of PGA corrected values for site effects).
 - 229 2. Count observed exceedances of PGA (after correcting the values for site effects) at PGA for 0.1g and 0.2g levels for
 230 each city complete time window and calculate their corresponding standard deviations considering the uncertainties
 231 in the intensity to PGA conversions.
 - 232 3. Calculate the predicted number of exceedances for each of the PGA thresholds considering every end-branch of the
 233 ESHM2022 logic tree (i.e., annual probability of exceedance × total time-period)
 - 234 4. Compute the weighted mean binomial distribution by combining all the binomial distributions applied to from (3)
 235 considering the full distribution of the hazard uncertainties. Calculate and calculate the probability (p-value) that the
 236 observed number of exceedances could be drawn from the weighted mean binomial distribution.
 - 237 5. Compute the p-value where there will be N observations or more than the observed number of exceedances from the
 238 weighted mean binomial distribution.

239 5 Statistical Testing Procedure: Results

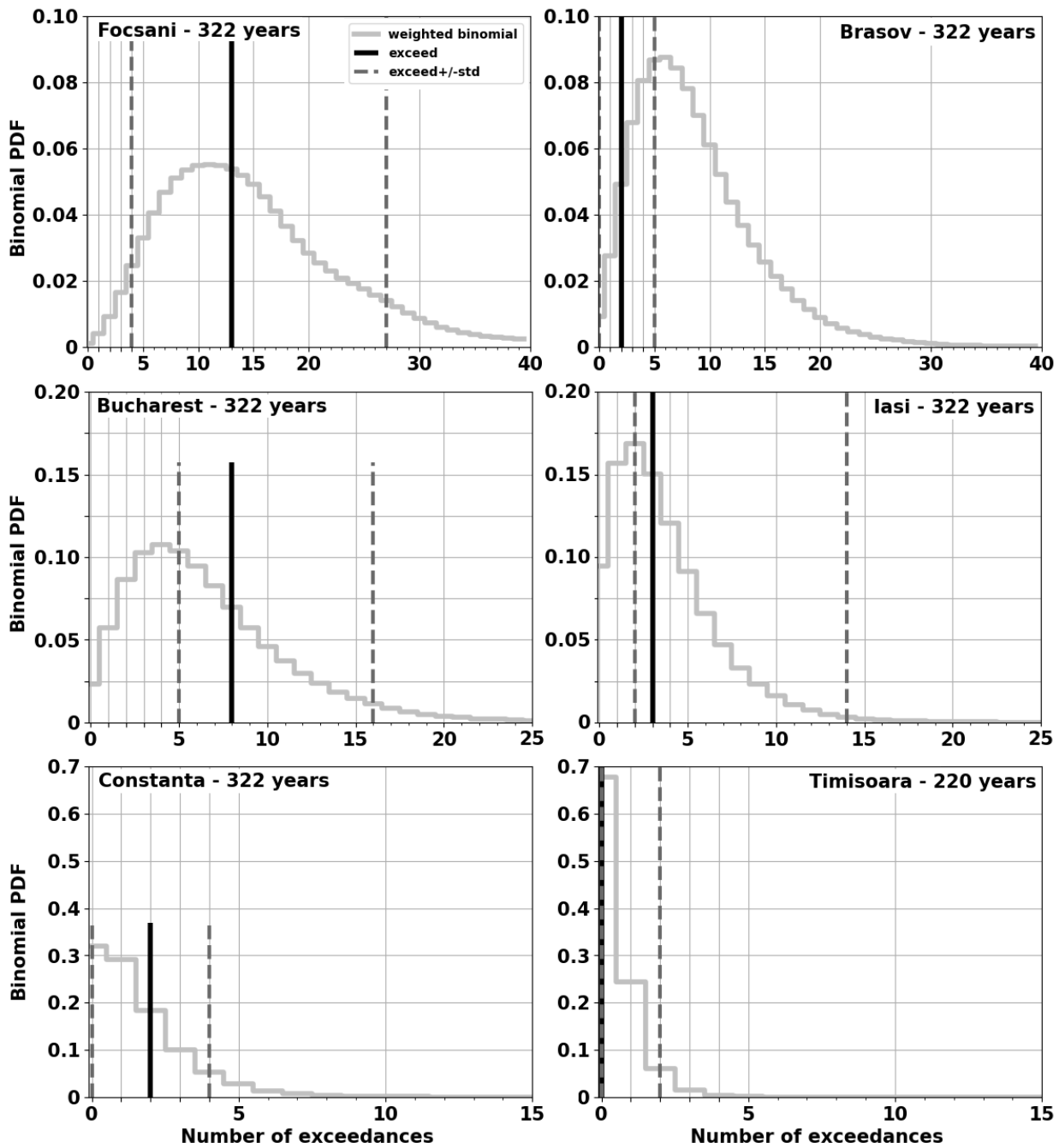
240 The results of the statistical testing of ESHM20 at 0.1 and 0.2g PGA are illustrated in *Figures 4* and *5* for six cities
241 (~~Focșani~~Focșani, Brașov, Bucharest, Iași, Constanța, and ~~Timișoara~~Timisoara), while for the others (Bacău, Câmpulung,
242 Cluj-Napoca, Craiova, Galați, Sibiu) are given in *Figures S2S3* and *S3S4* of the *Supplementary Materials*. These plots depict
243 the histogram of the weighted mean of ESHM20, the observed number of exceedances (i.e., black vertical line) and its one
244 sigma variability (i.e., dashed vertical lines). The total time of the observations is specified in each subplot for their respective
245 city. As mentioned before, the average time period of the observations of both ground shaking recordings and macroseismic
246 data spans over 322 years for all the cities, except the ones in the within the Carpathian region, such as: Sibiu and Cluj-Napoca,
247 as well as ~~Timișoara~~Timisoara, the westernmost city. For these cities, the time period is about 220 years. Overall, there is a
248 consistent alignment of estimated ground shaking hazard of ESHM20 with the observed data at 0.1g PGA level, as shown by
249 *Figure 5*. Notably, cities located along the northeast-southwest trajectory outside the Carpathians - such as Iași,
250 ~~Focșani~~Focșani, and Bucharest (see *Figure 4*) - show a robust correlation with the ESHM20 PGA estimates. Of particular
251 interest, ~~it's~~is the consistency of the ESHM20 with observations for ~~Focșani~~Focșani, the city found in the proximity of the Vrancea
252 deep seismicity sources, the main seismogenic source of the region. A slight shift from the ESHM20 prediction is observed in
253 the capital city of Romania, i.e., Bucharest, where ~~morean increased number of~~ intensities over VII MSK-64 were recorded
254 ~~than predicted; this fact and~~ might reflect the impact of the way humans experienced ground shaking within different typologies
255 of buildings in megacities (Rogozea, 2016; Cioflan et al., 2016). Also, such a shift might be attributed to the effect of different
256 source and path features, such as directivity, or uncertainties in correcting for site-effects. Furthermore, ~~the values expected~~
257 ~~from ESHM20 are over thean overestimation is~~ observed ~~ones~~ for cities along and in the proximity to the Carpathian bend,
258 e.g., Bacău, ~~Brașov~~Brasov and Câmpulung, and might suggest that a local attenuation effect is not currently captured or
259 modelled using the ESHM20 scaled backbone logic tree for the Vrancea in-slab region (Weatherill et al., 2020). The impact
260 of different attenuation patterns due to the complex tectonic configuration was previously seen on both human-felt and
261 instrumental observations (e.g, Radulian et al., 2006; Ivan, 2007; Marmureanu et al., 2016b) and captured within the recent
262 region-specific ground motion models (GMMs; e.g. Vacareanu et al., 2015; Manea et al., 2022). The results at the cities beyond
263 the Carpathian Mountains (e.g., Sibiu, Cluj-Napoca, ~~Timișoara~~Timisoara) exhibit hazard predictions that reflect the frequent
264 crustal seismic activity as a significant attenuation behind the arc ~~reducesdampened~~ VRI-related ground motion. It appears
265 that a longer and more comprehensive dataset may be required to accurately assess the distribution of ground shaking hazard
266 levels. For cities located in the far-field area of VRI and outside of the Carpathian arc (fore-arc region), such as Constanța and
267 Craiova, ~~an underprediction of the~~ ~~computed~~ hazard ~~is slightly lower than~~ ~~can be observed with respect to~~ the recorded data.
268 The same feature can be seen from the 475 return-period PGA map (see *Figure 1A*), and it contrasts with the recorded ground
269 motion field and pre-instrumental intensity data (e.g., Cioflan et al., 2022). Manea et al. (2022) provide insights of the apparent
270 attenuation of the ESHM20 ground motion model for the fore-arc area and future adjustments of the ESHM20 are
271 recommended to capture the ground motion characteristics within this region of Romania. However, the estimates of ESHM20

272 at 0.1g PGA appear overall to be ~~consistent in good agreement~~ to the data, ~~and~~ given all the uncertainties involved in this
273 analysis, ~~they are acceptable~~. Similarly, for the 0.2 g PGA level, the results suggest a strong correlation in areas near the VRI
274 source (see *Figure 5* and *Figure S4*). ~~As in the case of the 0.1g PGA level,~~ Focșani experiences multiple instances of
275 surpassing ~~the 0.1g~~ this PGA level; and the observed exceedances are ~~in good agreement~~ within the ESHM20 estimated
276 binomial distribution. Nevertheless, for the remaining cities, ESHM20 exceedances are ~~prone to slightly~~ ~~below~~ ~~underestimate~~
277 observed exceedances in Bucharest and Iasi, due to the influence of source/path effects and/or uncertainties in correcting for
278 site-effects. For the cities located along the Carpathian arc (Bacău, Brașov and Câmpulung), the trend is reversed, with
279 ESHM20 exceedances being higher than the observed ground shaking recurrences. For the rest of the cities (Galați, Craiova,
280 Timisoara Timisoara, Sibiu, Constanța, Cluj-Napoca), the ESHM20 estimates fit the observations relatively well. ~~The~~
281 ~~comparison~~ We also summarize the results as annual probabilities of exceedance at the two PGA levels (i.e., 0.1g and 0.2g) for
282 all the cities in *Figure S5* in the *Supplementary Materials*. ~~The observed consistency~~ between the ~~observations and the weighted~~
283 mean and the range of annual probabilities of exceedance from ESHM20 hazard curves ~~and those based on the observations~~
284 are consistent for the 0.1g PGA level. For the 0.2g PGA level, the consistency is valid for the cities located in the proximity
285 of the VRI. ~~Additionally, the measured and expected ESHM20 numbers of exceedances for each city are listed in Table 1~~
286 ~~together with their associated rate and probability of exceedances.~~
287 ~~The overall results are listed in Table 1 and the probability that the observed record could be drawn from the combined~~
288 ~~distribution (p-value) is presented at each location as “P 0.1” and “P 0.2”. These results show that nine out of twelve locations~~
289 ~~provide no evidence for poor performance of the ESHM20 for 0.1g PGA (poor performance - p-value < 0.05), while only at~~
290 ~~one location the hazard doesn’t pass the test at 0.2g. Overall, the testing results suggest that there are no reasons to reject the~~
291 ~~ESHM20 in Romania for 0.1 and 0.2g PGA.~~

292 6 Conclusions

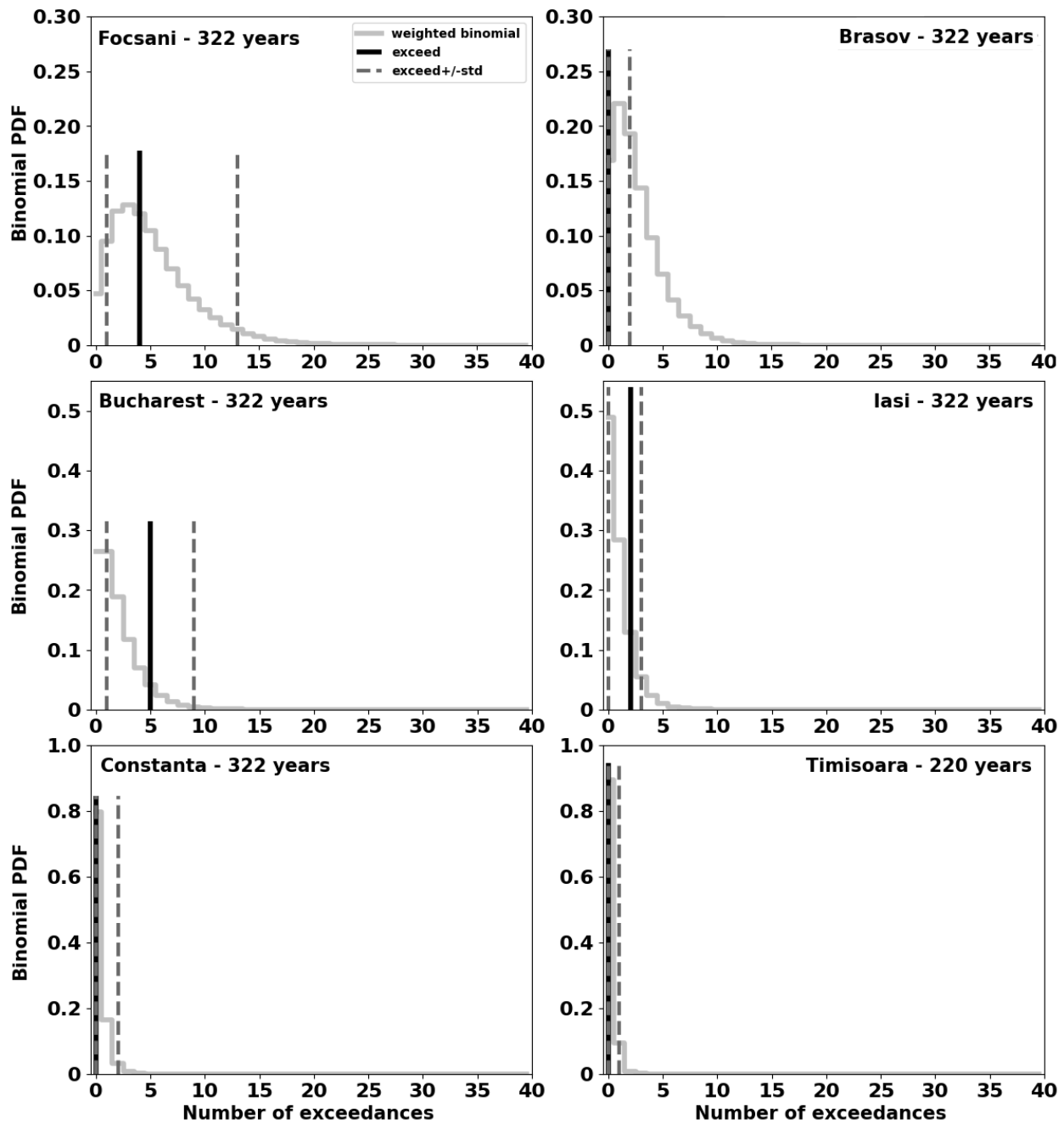
293 Evaluating the performance of seismic hazard models against recorded data, is an emerging research topic. In this study, we
294 evaluated the performance of the recent update of the ESHM20 (Danciu et al., 2021) in Romania. The compiled ground shaking
295 database combines strong motion records and macroseismic intensity data. The inclusion of the macroseismic intensity data,
296 allows expansion of the observational time period to over two to three hundred years, at the cost of increased uncertainties of
297 the ground motion estimates. The result of the statistical testing suggests that the ESHM20 is ~~consistent in a good agreement~~
298 with the observations for two PGA levels, at the locations of the twelve cities selected across Romania. We found a strong
299 ~~consistency agreement~~ between the weighted mean of ESHM20 and the exceedances of the observations for the cities (Focșani
300 and Galați) located in the proximity of the VRI source for both PGA levels i.e., 0.1g and 0.2g.
301 For cities located along the Carpathian arc (Bacău, Brașov Brașov and Câmpulung), the ESHM20 exceedances ~~are~~
302 ~~above~~ ~~appear to overestimate~~ the recorded ground motions and suggest that the along-arc attenuation effect (Manea et al., 2022)
303 might not be captured or modelled in the ESHM20 ground motion model (Weatherill et al., 2020). Furthermore, the testing

304 results at cities located in the VRI far-field area and outside of the Carpathian arc (Constanța, Craiova), might suggest that the
305 ground motion models used in ESHM20 attenuate too fast compared to the recorded PGA, as observed by Manea et al. (2022).
306 For the Iasi and Bucharest sites, located along the NE-SW direction from the VRI source, the ESHM20 ~~estimates appears to~~
307 ~~be below~~~~underestimates~~ the recorded data at the 0.1g PGA level and this feature become more prominent at 0.2 g; these
308 differences might be attributed to: 1) source directivity effects which are significant for major events occurring in Vrancea
309 ([Cioflan et al., 2022](#)), 2) potential bias in the conversion of the intensity to PGA, or 3) possible ~~complex~~ local site effects
310 which ~~might~~~~were~~ not ~~been completely~~ removed from the observations. While informative conclusions could be ~~drawn~~~~draw~~
311 from evaluating the comparison at cities along and outside of the Carpathian range, limited conclusions can be derived for
312 locations in regions of low seismic hazard, such as Sibiu and Cluj-Napoca, or ~~Timisoara~~~~Timisoara~~, in the western Romania.
313 The seismic hazard of these regions is dominated by episodic clusters of small to moderate shallow seismicity with regional
314 effects, which are not well captured in the macroseismic data or the amount of strong motion recordings. We acknowledge
315 that even with a time period of two to three centuries, the observations remain largely incomplete in time and space. The
316 Romanian seismic network (Marmureanu et al., ~~2021~~~~2022~~) has evolved over time, however limited ground motion data is
317 available due to lack of significant earthquakes occurring in the recent decade or so. Uncertainties associated with the ground
318 motion dataset are increasing with the conversion of the macroseismic data, as illustrated in the results given in *Figures 4* and
319 *5*. Moreover, ~~we also acknowledge that~~ the statistical testing ~~is~~~~are~~ limited in scope given all the uncertainties are associated
320 also with the distribution of the hazard results, configuration of the logic tree, sampling technique, and/or use of a certain
321 distribution i.e., binomial or log-normal. All these factors are contributing to the overall stability of the statistical testing.
322 In conclusion, our analysis suggests that observed exceedance rates for these two PGA levels, i.e., 0.1g and 0.2g, are consistent
323 with ESHM20 estimates. ~~These, but these~~ results must be interpreted with caution given the ~~above mentioned~~~~above-mentioned~~
324 limitations in ~~the~~ time and spatial coverage of the observations, both the ground shakings and the macroseismic intensity
325 dataset.



326

327 Figure 4. Consistency test results of ESHM20 with the observed PGA values at 0.1 g for each of six cities: Focsani, Brasov,
 328 Bucharest, Iasi, Constanta, and Timisoara. The histogram depicts the ESHM20 weighted mean, the observed number of
 329 exceedances over the time window of completeness is given as the black vertical line and its one sigma variability i.e., dashed
 330 vertical lines; the total completeness time is specified in each subplot for their respective city.



331
 332
 333
 334
 335
 336
 337

Figure 5. Consistency test results of ESHM20 with the observed PGA values at 0.2 g for six representative cities. The histogram depicts the ESHM20 weighted mean-predicted histogram, the observed number of exceedances over the time window of completeness is given as the black vertical line and its one sigma variability i.e., dashed vertical lines; the total completeness time is specified in each subplot for their respective city.

338
339
340
341

Table 1. Observed and [the](#) ESHM 2020 predicted exceedances for 0.1 and 0.2g PGA at twelve [Romanian](#) cities.

City	T	SC	N 0.1	Rate 0.1	APE 0.1	P 0.1	P> 0.1	N 0.2	Rate 0.2	APE 0.2	P 0.2	P> 0.2
Bacău	322	C	4	0.01242	0.01235	0.06551	0.88613	2	0.00621	0.00619	0.12691	1.00000
Braşov	322	B	2	0.00621	0.00619	0.04927	0.96333	1	0.00311	0.00310	0.16854	1.00000
Bucharest	322	C	8	0.02484	0.02454	0.06947	0.34191	5	0.01553	0.01541	0.04063	0.09541
Câmpulung	322	B	1	0.00311	0.00310	0.04146	0.98512	1	0.00311	0.00310	0.21444	1.00000
Cluj-Napoca	284	B	1	0.00352	0.00351	0.13002	0.14835	1	0.00352	0.00351	0.95985	1.00000
Constanţa	322	C	2	0.00621	0.00619	0.18241	0.38990	1	0.00311	0.00310	0.79675	1.00000
Craiova	322	C	3	0.00932	0.00927	0.08392	0.16519	1	0.00311	0.00310	0.82129	1.00000
Focşani	322	C	13	0.04037	0.03957	0.05461	0.55554	4	0.01242	0.01235	0.11991	0.60844
Galaţi	322	B	4	0.01242	0.01235	0.09490	0.78712	1	0.00311	0.00310	0.24510	0.77985
Iaşi	322	B	3	0.00932	0.00927	0.15007	0.58011	2	0.00621	0.00619	0.12878	0.22567
Sibiu	250	B	1	0.00400	0.00399	0.30161	0.48469	1	0.00400	0.00399	0.87168	1.00000
Timişoara	220	B	1	0.00455	0.00454	0.67819	1.00000	1	0.00455	0.00454	0.89580	1.00000

342
343
344
345
346
347
348
349
350
351
352

[Where:](#)

[T = time window of completeness \[years\];](#)

[SC = EC8 site class \(CEN, 2004\);](#)

[N 0.1 \(N 0.2\) = number of observed exceedances in T for 0.1 \(0.2\) g PGA;](#)

[Rate 0.1 \(Rate 0.2\) = observed annual rate of exceedance for 0.1 \(0.2\) g PGA;](#)

[APE 0.1 \(APE 0.2\) = Annual probability of exceedance for 0.1g - calculated from observed rate;](#)

[P 0.1 \(P0.2\) = P-value that the observed number of exceedances within T could be drawn from ESHM20 for 0.1 \(0.2\) g;](#)

[P>0.1 \(P>0.2\) = P-value where there will be N observations or more than the observed number of exceedances within T from ESHM20 for 0.1 \(0.2\) g PGA](#)

353

354 **Supplementary Material**

355 The electronic Supplement contains additional plots of the distribution of the MSK-64 Intensity to PGA conversions for the
356 two selected equations, the ESHM20 annual probability of exceedance distribution for Bucharest, the testing results for six
357 cities and a summary plot of the results at all the locations.

358 **Data availability**

359 The collected intensity data can be made available by the authors only upon request as this study was done ~~within~~ withing an
360 ongoing project. The OpenQuake Engine input files and running scripts for ESHM20 can be downloaded from:
361 <https://gitlab.seismo.ethz.ch/efehr>.

362 **Author contributions**

363 EFM, LD and CCO designed the framework of the work. EFM, LD and MG developed the codes and performed the testing
364 analysis. CCO and DTD collected and harmonised the intensity data. EM and LD designed and wrote the paper with
365 contributions from the other co-authors.

366

367 **Competing interests**

368 The authors declare that they have no conflict of interests.

369

370 **Acknowledgments**

371 This study was carried out within the National Research Program SOL4RISC Grant No. 24N/2023, project no. PN23360202.
372 The second author received support and resources from Geo-INQUIRE Project, Grant agreement ID: 1010585182,
373 DOI10.3030/101058518. The seismic hazard calculations at the selected locations were performed using the OpenQuake
374 Engine version 3.14 (DOI 10.13117/openquake.engine, last accessed 01.06.2023). The software suite ArcGis
375 (www.esri.com/software/arcgis, last accessed 01.03.2023) was used for mapping and all the plots were done with Python using
376 open-source libraries. Part of the python investigation codes were developed within the New Zealand National Seismic Hazard
377 Model 2022 Revision Project (contract 2020-BD101).

379 **References**

- 380 Allen, T.I., Ghasemi, H, and Griffin, J.D.: Exploring Australian hazard map exceedance using an Atlas of historical
 381 ShakeMaps. *Earthquake Spectra*, 39(2), 985-1006, doi:10.1177/87552930231151977, 2023.
- 382 Ardeleanu, L., Leydecker, G., Bonjer, K.-P., Busche, H., Kaiser, D., and Schmitt, T.: Probabilistic seismic hazard map for
 383 Romania as a basis for a new building code, *Nat. Hazards Earth Syst. Sci.*, 5, 679–684, doi: 10.5194/nhess-5-679-2005.
- 384 Atanasiu, I.: *Cutremurele de pamant din Romania*, Ed. Academiei Romane, 196 p, Bucharest, 1961.
- 385 Caprio, M., Tarigan, B., Worden, C. B., Wiemer, S., & Wald, D. J.: Ground Motion to Intensity Conversion Equations
 386 (GMICES): A Global Relationship and Evaluation of Regional Dependency. *Bulletin of the Seismological Society of America*,
 387 105 (3): 1476–1490. doi: <https://doi.org/10.1785/0120140286>, 2015.
- 388 Cioflan, C. O., Manea, E. F., & Apostol, B. F. (2022). Insights from neo-deterministic seismic hazard analyses in Romania. In
 389 *Earthquakes and sustainable infrastructure*, p. 415-432, Elsevier, <https://doi.org/10.1016/B978-0-12-823503-4.00013-0>, 2022.
- 390 Cioflan, C.O., Toma-Danila, D., and Manea, E.F.: Seismic Loss Estimates for Scenarios of the 1940 Vrancea Earthquake. In:
 391 Vacareanu, R., Ionescu, C. (eds) *The 1940 Vrancea Earthquake. Issues, Insights and Lessons Learnt*. Springer Natural Hazards.
 392 Springer, Cham. https://doi.org/10.1007/978-3-319-29844-3_30, 2016.
- 393 Coman, A., Manea, E. F., Cioflan, C. O., & Radulian, M.: Interpreting the fundamental frequency of resonance for
 394 Transylvanian Basin. *Romanian Journal of Physics*, 65, 809, 2020.
- 395 Comité Européen de Normalisation (CEN): Eurocode 8, design of structures for earthquake resistance—Part 1: General rules,
 396 seismic actions and rules for buildings. European Standard NF EN 1998-1. Brussels: CEN, 2004.
- 397 Constantin A. P., Pantea A., Stoica R.: Vrancea (Romania) Subcrustal Earthquakes: Historical Sources and Macroseismic
 398 Intensity Assessment, *Romanian Journal of Physics*, 56, 5-6, p. 813 – 826, 2011.
- 399 Constantin, A. P., Moldovan, I. A., Craiu, A., Radulian, M., and Ionescu, C.: Macroseismic intensity investigation of the
 400 November 2014, M=5.7, Vrancea (Romania) crustal earthquake, *Annals of Geophysics*, 59, 5, doi:10.4401/ag-6998, 2016.
- 401 Constantin, A., Manea, L., Diaconescu, M., & Moldovan, I.: Intensity and macroseismic maps of the latest moderate sized
 402 Vrancea earthquakes. *Romanian Reports in Physics*, 75, 702, 2023.
- 403 Constantin, A.P., Pantea, A. Macroseismic field of the October 27, 2004 Vrancea (Romania) moderate subcrustal earthquake.
 404 *J Seismol* 17, 1149–1156, <https://doi.org/10.1007/s10950-013-9383-2>, 2013.
- 405 Craiu, A., Ferrand, T. P., Manea, E. F., Vrijmoed, J. C., and Mărmureanu, A.: A switch from horizontal compression to vertical
 406 extension in the Vrancea slab explained by the volume reduction of serpentine dehydration. *Sci Rep* 12, 22320,
 407 <https://doi.org/10.1038/s41598-022-26260-5>, 2022.
- 408 [Craiu, A., Craiu, M., Mihai, M., Manea, E. F., & Marmureanu, A. \(2023\). Vrancea intermediate-depth focal mechanism](#)
 409 [catalog: a useful instrument for local and regional stress field estimation. *Acta Geophysica*, 71\(1\), 29-52.](#)

410 Danciu, L., Nandan, S., Reyes, C., Basili, R., Weatherill, G., Beauval, C., Rovida A., Vilanova, S., Sesetyan, K., Bard, P-
411 Y., Cotton, F., Wiemer, S., and Giardini, D.: The 2020 update of the European Seismic Hazard Model: Model
412 Overview. EFER Technical Report 001, v1.0.0, <https://doi.org/10.12686/a15>, 2021.

413 Danciu, L., Weatherill, G., Rovida, A., Basili, R., Bard, P.Y., Beauval, C., Nandan, S., Pagani, M., Crowley, H., Sesetyan, K.,
414 Villanova, S., Reyes, C., Marti, M., Cotton, F., Wiemer, S., and Giardini, D.: The 2020 European Seismic Hazard Model:
415 Milestones and Lessons Learned. In: Vacareanu, R., Ionescu, C. (eds) Progresses in European Earthquake Engineering and
416 Seismology. ECEES 2022. Springer Proceedings in Earth and Environmental Sciences. Springer, Cham.
417 https://doi.org/10.1007/978-3-031-15104-0_1, 2022.

418 [Danciu, L., Giardini, D., Weatherill, G., Basili, R., Nandan, S., Rovida, A., Beauval, C., Bard, P.-Y., Pagani, M., Reyes, C.,
419 G., Sesetyan, K., Vilanova, S., Cotton, F., and Wiemer, S.: The 2020 European Seismic Hazard Model: Overview and Results,
420 EGU sphere \[preprint\]. <https://doi.org/10.5194/egusphere-2023-3062>, 2024.](https://doi.org/10.5194/egusphere-2023-3062)

421 Ferrand, T.P., Manea, E.F.: Dehydration-induced earthquakes identified in a subducted oceanic slab beneath Vrancea,
422 Romania. Sci Rep 11, 10315. <https://doi.org/10.1038/s41598-021-89601-w>, 2021.

423 [Gerstenberger, Matthew C., Warner Marzocchi, Trevor Allen, Marco Pagani, Janice Adams, Laurentiu Danciu, Edward H.
424 Field et al.: Probabilistic seismic hazard analysis at regional and national scales: State of the art and future challenges. *Reviews
425 of Geophysics* 58, no. 2 \(2020\): e2019RG000653.](https://doi.org/10.1002/2014EO290001)

426 Giardini, D., Wössner, J., and Danciu, L.: Mapping Europe's seismic hazard. Eos, Transactions American Geophysical Union,
427 95, 29, 261-262, <https://doi.org/10.1002/2014EO290001>, 2014.

428 Hanks, T. C., Beroza, G. C., & Toda, S.: Have recent earthquakes exposed flaws in or misunderstandings of probabilistic
429 seismic hazard analysis?. *Seismological Research Letters*, 83(5), 759-764, doi: <https://doi.org/10.1785/0220120043>, 2012.

430 Iervolino I., Chioccarelli E., Cito P.: Testing three seismic hazard models for Italy via multi-site observations. PLoS ONE
431 18(4): e0284909, <https://doi.org/10.1371/journal.pone.0284909>, 2023.

432 Ivan, M.: Attenuation of P and pP waves in Vrancea area–Romania. *Journal of seismology*, 11(1), 73-85,
433 <https://doi.org/10.1007/s10950-006-9038-7>, 2007.

434 Kronrod, T., Radulian, M., Panza, G., Popa, M., Paskaleva, I., Radovanovich, S., Gribovski, K., Sandu, I., and Pekevski, L.:
435 Integrated transnational macroseismic data set for the strongest earthquakes of Vrancea (Romania), *Tectonophysics*, 590, 1-
436 23, doi: 10.1016/j.tecto.2013.01.019, 2013.

437 Mak, S., Schorlemmer, D.: A Comparison between the Forecast by the United States National Seismic Hazard Maps with
438 Recent Ground-Motion Records. *Bulletin of the Seismological Society of America*; 106 (4): 1817–1831. doi:
439 <https://doi.org/10.1785/0120150323>, 2016.

440 Manea, E. F., Predoiu, A., Cioflan, C. O., & Diaconescu, M.: Interpretation of resonance fundamental frequency for Moldavian
441 and Scythian platforms. *Romanian Reports in Physics*, 71, 709, 2019.

442 Manea, E.F., Cioflan, C. O., and Danciu, L.: Ground-motion models for Vrancea intermediate-depth earthquakes. *Earthquake
443 Spectra*, 38, 1, 407-431, doi:10.1177/87552930211032985, 2022.

444 Marmureanu, G., Cioflan, C.O. and Marmureanu, A.: Intensity seismic hazard map of Romania by probabilistic and (neo)
445 deterministic approaches, linear and nonlinear analyses, *Rom. Rep. Phys.*, 63(1), 226-239, 2011.

446 Marmureanu, G., Cioflan, C.O., Marmureanu, A., and Manea, E.F.: Main Characteristics of November 10, 1940 Strong
447 Vrancea Earthquake in Seismological and Physics of Earthquake Terms. In: Vacareanu, R., Ionescu, C. (eds) *The 1940 Vrancea*
448 *Earthquake. Issues, Insights and Lessons Learnt*. Springer Natural Hazards. Springer, Cham. [https://doi.org/10.1007/978-3-](https://doi.org/10.1007/978-3-319-29844-3_5)
449 [319-29844-3_5](https://doi.org/10.1007/978-3-319-29844-3_5), 2016b.

450 Marmureanu, G., Marmureanu, A., Manea, E.F., Toma-Danila, D., and Vlad, M.: Can we still use classic seismic hazard
451 analysis for strong and deep Vrancea earthquakes. *Romanian Reports in Physics*, 61(3–4), 728-738, 2016a.

452 Marmureanu, G., [Manea, E. F., Cioflan, C. O., Marmureanu, A., & Toma-Danila, D.: Spectral response features used in last](#)
453 [IAEA stress test to NPP Cernavoda \(ROMANIA\) by considering strong nonlinear behaviour of site soils. *Romanian Journal*](#)
454 [of Physics](#), 62, 822, 2017.

455 [Marmureanu, G.](#) Vacareanu, R., Cioflan, C.O., Ionescu, C., and Toma-Danila, D.: Historical Earthquakes: New Intensity Data
456 Points Using Complementary Data from Churches and Monasteries (chapter). *Seismic Hazard and Risk Assessment. Updated*
457 *Overview with Emphasis on Romania*. Ed: Vacareanu R., Ionescu C., Springer Natural Hazards, Springer International
458 Publishing, doi: 10.1007/978-3-319-74724-8_7, 2018.

459 [Mărmureanu, A., Ionescu, C., Grecu, B., Toma-Danila, D., Tigănescu, A., Neagoe, C., ... & Ilieș, I.: From national to](#)
460 [transnational seismic monitoring products and services in the Republic of Bulgaria, Republic of Moldova, Romania, and](#)
461 [Ukraine. *Seismological Society of America*, 92\(3\), 1685-1703, 2021.](#)

462 Marzocchi, W., and Jordan, T. H.: Experimental concepts for testing probabilistic earthquake forecasting and seismic hazard
463 models. *Geophysical Journal International*, 215, 2, 780-798, <https://doi.org/10.1093/gji/ggy276>, 2018.

464 Marzocchi, W., and Jordan, T.H.: A unified probabilistic framework for seismic hazard analysis, *Bull. Seismol. Soc. Am.*,
465 107(6), 2738-2744, <https://doi.org/10.1785/0120170008>, 2017.

466 Marzocchi, W., and Jordan, T.H.: Testing for ontological errors in probabilistic forecasting models of natural systems, *Proc.*
467 *Natl. Acad. Sci.*, 111(33), 11973- 11978, <https://doi.org/10.1073/pnas.1410183111>, 2014.

468 Medvedev, S.V., Sponheuer, W. and Karnik, V.: Seismic intensity scale version MSK 1964, *Publ. Inst. Geodynamik*, 48, Jena
469 48, 1967.

470 Meletti, C., Marzocchi, W., D'Amico, V., and Lanzano, G., The new Italian seismic hazard model (MPS19). *Annals of*
471 *Geophysics* 64(1), DOI:10.4401/ag-8579, 2021.

472 Mousavi, S.M., Beroza, G.C.: Evaluating the 2016 One-Year Seismic Hazard Model for the Central and Eastern United States
473 Using Instrumental Ground-Motion Data. *Seismological Research Letters* 89 (3): 1185–1196. doi:
474 <https://doi.org/10.1785/0220170226>, 2018.

475 Musson, R.M.W., Grünthal, G., and Stucchi, M.: The comparison of macroseismic intensity scales. *Journal of Seismology*, 14,
476 413-428, <https://doi.org/10.1007/s10950-009-9172-0>, 2010.

477 Oncescu, M.C., Marza, V.I., Rizescu, M., Popa, M.: The Romanian earthquake catalogue between 984–1997. In “Vrancea
478 Earthquakes: Tectonics, Hazard and Risk Mitigation: Contributions from the First International Workshop on Vrancea
479 Earthquakes”, Bucharest, Romania, November 1–4, 1997, pp. 43-47. https://doi.org/10.1007/978-94-011-4748-4_4, 1999.

480 Pagani, M., Monelli, D., Weatherill, G., Danciu, L., Crowley, H., Silva, V., ... & Simionato, M.: OpenQuake engine: An open
481 hazard (and risk) software for the global earthquake model. *Seismological Research Letters*, 85(3), 692-702, doi:
482 <https://doi.org/10.1785/0220130087>, 2014.

483 Radu, C.: Catalogue of Strong Earthquakes Originated on the Romanian Teritmt T, Part I: Before 1901. In *Seismological
484 Researches on the Earthquake of March 4, 1977*, Monograph (eds. Cornea, I. and Radu, C.) (Central Institute of Physics,
485 Bucharest), 1979.

486 Radulian, M., Panza, G. F., Popa, M., & Grecu, B.: Seismic wave attenuation for Vrancea events revisited. *Journal of
487 Earthquake Engineering*, 10(03), 411-427, <https://doi.org/10.1080/13632460609350603>, 2006.

488 Rey, J., Beauval, C., and Douglas, J.: Do French macroseismic intensity observations agree with expectations from the
489 European Seismic Hazard Model 2013?, *Journal of Seismology*, 22, 589-604, <https://doi.org/10.1007/s10950-017-9724-7>,
490 2018.

491 Rogozea M., Marmureanu G., Radulian M., Toma D.: Reevaluation of the macroseismic effects of the 23 January 1838
492 Vrancea earthquake. *Romanian Reports in Physics*, 66(2):520-538, 2014.

493 Rogozea M.: *Impactul cutremurelor majore din România: trecut, prezent și viitor*. Editura Electra, București, 2016.

494 Rovida A., Albin P., Locati M., Antonucci A.: Insights into Preinstrumental Earthquake Data and Catalogs in Europe.
495 *Seismological Research Letters*, 91(5), 2546–2553, <https://doi.org/10.1785/0220200058>, 2020.

496 Salditch, L., Gallahue, M. M., Lucas, M. C., Neely, J. S., Hough, S. E., and Stein, S.: California Historical Intensity Mapping
497 Project (CHIMP): A consistently reinterpreted dataset of seismic intensities for the past 162 yr and implications for seismic
498 hazard maps. *Seismological Research Letters*, 91(5), 2631-2650, doi: <https://doi.org/10.1785/0220200065>, 2020.

499 Shebalin N.V., Karnik V., Hadzievski D.: UNDP-Unesco Survey of the Seismicity of Balkan Region. *Catalogue of earthquakes
500 of the Balkan region*. Printing Office of the University Kiril and Metodij, Skopje, 599p., 1974.

501 Sibson, R.: A Brief Description of Natural Neighbor Interpolation. In: Barnett, V., Ed., *Interpreting Multivariate Data*, John
502 Wiley & Sons, New York, 21-36, 1981.

503 Sokolov, V. Y., Wenzel, F., and Mohindra, R.: Probabilistic seismic hazard assessment for Romania and sensitivity analysis:
504 a case of joint consideration of intermediate-depth (Vrancea) and shallow (crustal) seismicity, *Soil Dynamics and Earthquake
505 Engineering*, 29(2), 364-381. <https://doi.org/10.1016/j.soildyn.2008.04.004>, 2009.

506 Sokolov, V., Bonjer, K. P., Wenzel, F., Grecu, B., and Radulian, M.: Ground-motion prediction equations for the intermediate
507 depth Vrancea (Romania) earthquakes. *Bull Earthquake Eng* 6, 367–388 <https://doi.org/10.1007/s10518-008-9065-6>, 2008.

508 Stirling, M., Manea, E., Gerstenberger, M., & Bora, S.: Testing and Evaluation of the New Zealand National Seismic Hazard
509 Model 2022. *Bulletin of the Seismological Society of America*, doi: <https://doi.org/10.1785/0120230108>, 2023.

510 Stirling, M.W., and Gerstenberger, M.C.: Ground motion-based testing of seismic hazard models in New Zealand. *Bulletin of*
511 *the Seismological Society of America*, 100(4): 1407-1414; doi: 10.1785/0120090336, 2010.

512 Tasan, H., Beauval, C., Helmstetter, A., Sandikkaya, A., & Guéguen, P: Testing probabilistic seismic hazard estimates against
513 accelerometric data in two countries: France and Turkey. *Geophysical Journal International*, 198(3), 1554-1571. doi:
514 <https://doi.org/10.1093/gji/ggu191>, 2014.

515 Vacareanu, R., Iancovici, M., Neagu, C., and Pavel, F.: Macroseismic intensity prediction equations for Vrancea intermediate-
516 depth seismic source, *Natural Hazards*, 79(3), 2005-2031, <https://doi.org/10.1007/s11069-015-1944-y>, 2015.

517 Vacareanu, R., Marmureanu, G., Pavel, F., Neagu, C., Cioflan, C. O., and Aldea, A.: Analysis of soil factor S using strong
518 ground motions from Vrancea subcrustal seismic source. *Rom Rep Phys*, 66(3), 893-906, 2014.

519 Vanneste, K., Stein, S., Camelbeeck, T., and Vleminckx, B.: Insights into earthquake hazard map performance from shaking
520 history simulations. *Scientific reports*, 8(1), 1855, <https://doi.org/10.1038/s41598-018-20214-6> , 2018.

521 Weatherill, G., Kotha, S. R., & Cotton, F.: A regionally-adaptable “scaled backbone” ground motion logic tree for shallow
522 seismicity in Europe: application to the 2020 European seismic hazard model. *Bulletin of Earthquake Engineering*, 18(11),
523 5087-5117, <https://doi.org/10.1007/s10518-020-00899-9>, 2020.

524 Weatherill, G., Kotha, S. R., Danciu, L., Vilanova, S., and Cotton, F.: Modelling seismic ground motion and its uncertainty in
525 different tectonic contexts: Challenges and application to the 2020 European Seismic Hazard Model (ESHM20). *Natural*
526 *Hazards and Earth System Sciences*, Preprint nhess-2023-124, 1-66, <https://doi.org/10.5194/nhess-2023-124>, 2023.